

000  
 001  
 002  
 003  
 004 **Supplementary Material to “External Prior Guided Internal Prior Learning for**  
 005 **Real Noisy Image Denoising”**  
 006  
 007  
 008  
 009  
 010  
 011  
 012  
 013  
 014  
 015  
 016  
 017  
 018  
 019  
 020  
 021  
 022  
 023  
 024  
 025  
 026  
 027  
 028  
 029  
 030  
 031  
 032  
 033  
 034  
 035  
 036  
 037  
 038  
 039  
 040  
 041  
 042  
 043  
 044  
 045  
 046  
 047  
 048  
 049  
 050  
 051  
 052  
 053  
 054  
 055  
 056  
 057  
 058  
 059  
 060  
 061  
 062  
 063  
 064  
 065  
 066  
 067  
 068  
 069  
 070  
 071  
 072  
 073  
 074  
 075  
 076  
 077  
 078  
 079  
 080  
 081  
 082  
 083  
 084  
 085  
 086  
 087  
 088  
 089  
 090  
 091  
 092  
 093  
 094  
 095  
 096  
 097  
 098  
 099  
 100  
 101  
 102  
 103  
 104  
 105  
 106  
 107

Anonymous CVPR submission

Paper ID 1047

In this supplementary material, we provide:

1. The closed-form solution of the sparse coding problem (6) in the main paper.
2. More denoising results on the real noisy images (with no “ground truth”) provided in the dataset [1].
3. More denoising results on the 15 cropped real noisy images (with “ground truth”) used in the dataset [2].
4. More denoising results on the 60 cropped real noisy images (with “ground truth”) from [2].

## 1. Closed-Form Solution of the Weighted Sparse Coding Problem (6)

For notation simplicity, we ignore the index  $n, m, t$  in the sparse coding problem (6) in the main paper. And it turns into the following weighted sparse coding problem:

$$\min_{\alpha} \|\mathbf{y} - \mathbf{D}\alpha\|_2^2 + \sum_{j=1}^{3p^2} \lambda_j |\alpha_j|. \quad (1)$$

Since  $\mathbf{D}$  is an orthogonal matrix, problem (1) is equivalent to

$$\min_{\alpha} \|\mathbf{D}^T \mathbf{y} - \alpha\|_2^2 + \sum_{j=1}^{3p^2} \lambda_j |\alpha_j|. \quad (2)$$

For simplicity, we denote  $\mathbf{z} = \mathbf{D}^T \mathbf{y}$ . Here we have  $\lambda_j \geq 0, j = 1, \dots, 3p^2$ , then problem (2) can be written as

$$\min_{\alpha} \sum_{j=1}^{3p^2} ((\mathbf{z}_j - \alpha_j)^2 + \lambda_j |\alpha_j|). \quad (3)$$

The problem (3) is separable w.r.t. each  $\alpha_j$  and hence can be simplified to  $3p^2$  independent scalar minimization problems

$$\min_{\alpha_j} (\mathbf{z}_j - \alpha_j)^2 + \lambda_j |\alpha_j|, \quad (4)$$

where  $j = 1, \dots, 3p^2$ . Taking derivative of  $\alpha_j$  in problem (4) and setting the derivative to be zero. There are two cases for the solution.

- (a) If  $\alpha_j \geq 0$ , we have

$$2(\alpha_j - \mathbf{z}_j) + \lambda_j = 0. \quad (5)$$

The solution is

$$\hat{\alpha}_j = \mathbf{z}_j - \frac{\lambda_j}{2} \geq 0. \quad (6)$$

So  $\mathbf{z}_j \geq \frac{\lambda_j}{2} > 0$ , and the solution  $\hat{\alpha}_j$  can be written as

$$\hat{\alpha}_j = \text{sgn}(\mathbf{z}_j) * (|\mathbf{z}_j| - \frac{\lambda_j}{2}), \quad (7)$$

where  $\text{sgn}(\bullet)$  is the sign function.

- (b) If  $\alpha_j < 0$ , we have

$$2(\alpha_j - \mathbf{z}_j) - \lambda_j = 0. \quad (8)$$

The solution is

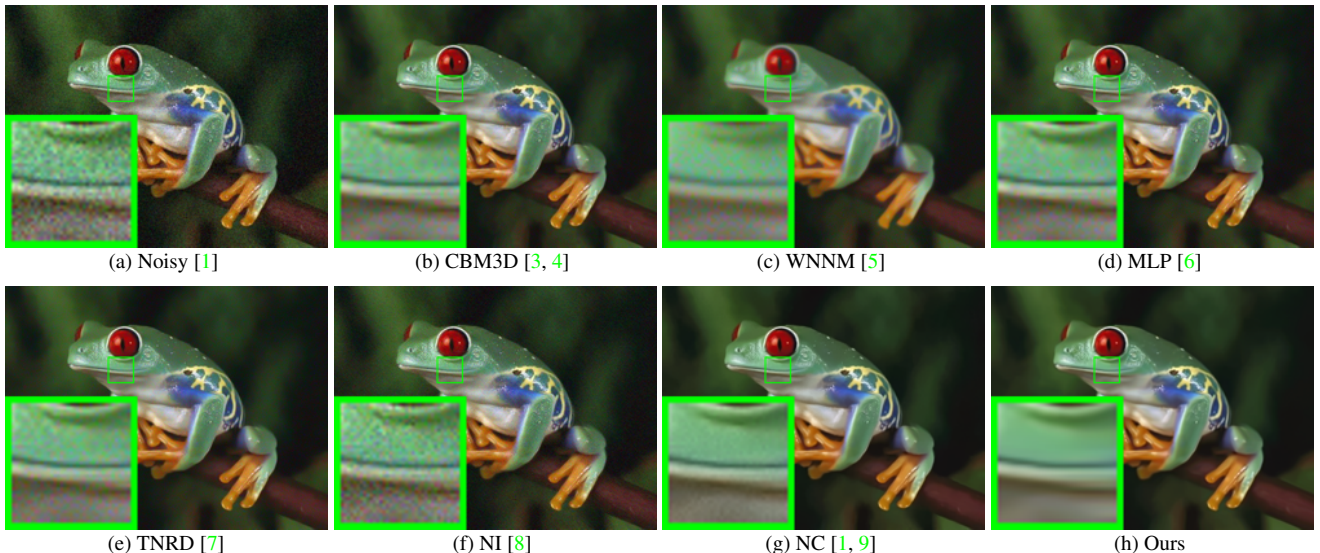
$$\hat{\alpha}_j = \mathbf{z}_j + \frac{\lambda_j}{2} < 0. \quad (9)$$

108 So  $\mathbf{z}_j < -\frac{\lambda_j}{2} < 0$ , and the solution  $\hat{\alpha}_j$  can be written as 162  
 109  
 110 
$$\hat{\alpha}_j = \text{sgn}(\mathbf{z}_j) * (-\mathbf{z}_j - \frac{\lambda_j}{2}) = \text{sgn}(\mathbf{z}_j) * (|\mathbf{z}_j| - \frac{\lambda_j}{2}).$$
 163  
 111

112 In summary, we have the final solution of the weighted sparse coding problem (1) as 164  
 113  
 114 
$$\hat{\alpha} = \text{sgn}(\mathbf{D}^T \mathbf{y}) \odot \max(|\mathbf{D}^T \mathbf{y}| - \lambda/2, 0),$$
 165  
 115 where  $\odot$  means element-wise multiplication and  $|\mathbf{D}^T \mathbf{y}|$  is the absolute value of each entry of the vector  $\mathbf{D}^T \mathbf{y}.$  166  
 116

## 2. More Results on Real Noisy Images in [1]

118 In this section, we give more visual comparisons of the competing methods on the real noisy images provided in [1]. The 172  
 119 real noisy images in this dataset [1] have no “ground truth” images and hence we only compare the visual quality of the 173  
 120 denoised images by different methods. As can be seen from Figures 1-4, our proposed method performs better than the state- 174  
 121-of-the-art denoising methods. This validates the effectiveness of our proposed external prior guided internal prior learning 175  
 122 framework for real noisy image denoising. 176  
 123



142 Figure 1. Denoised images of the real noisy image “Frog” [1] by different methods. The images are better to be zoomed in on screen. 196  
 143  
 144

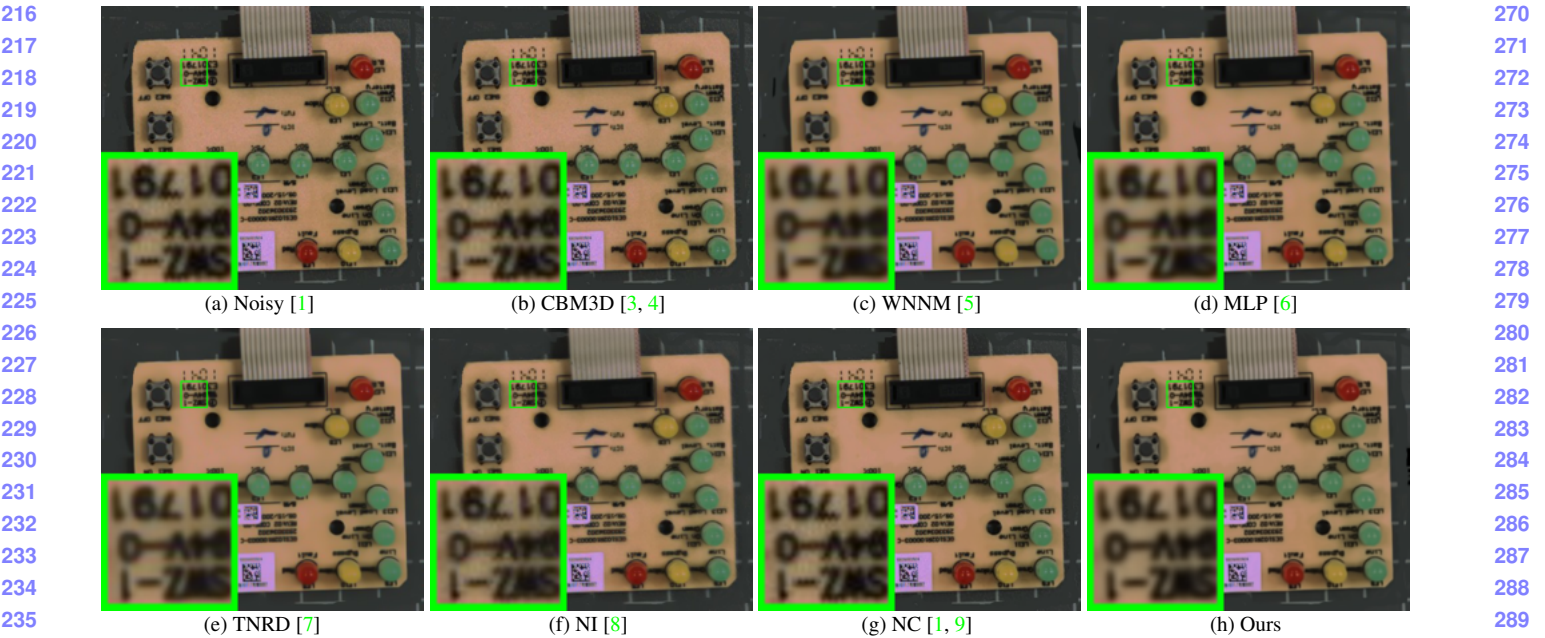


Figure 2. Denoised images of the real noisy image “Circuit” [1] by different methods. The images are better to be zoomed in on screen.

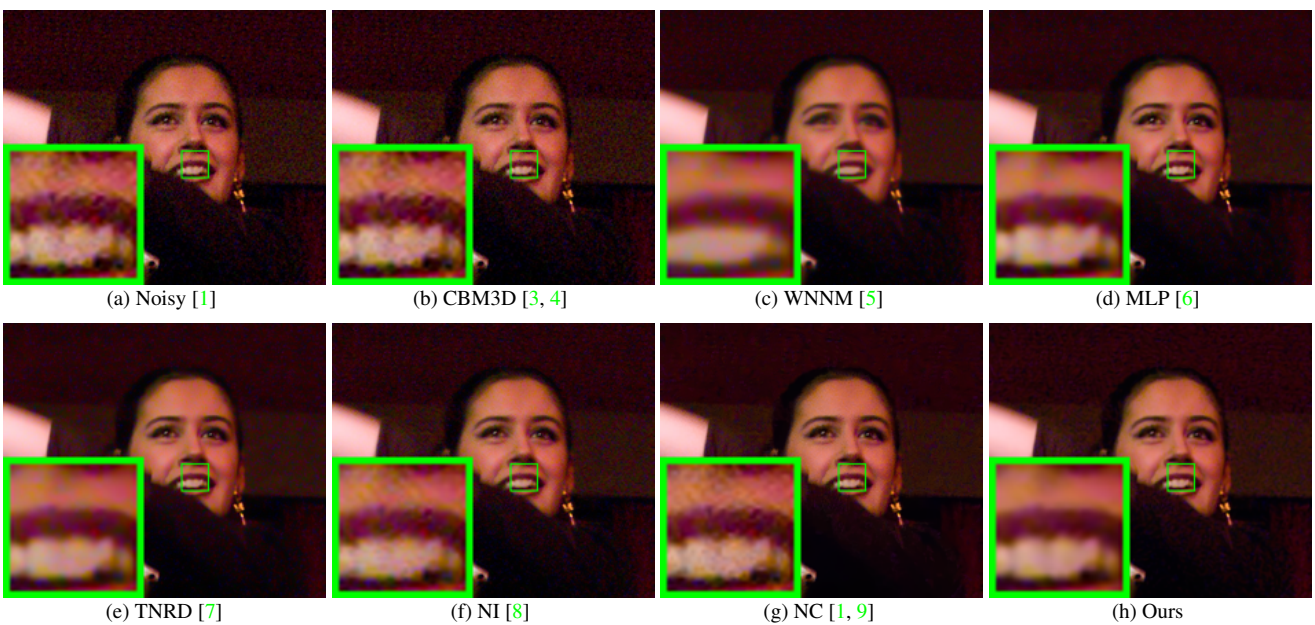


Figure 3. Denoised images of the real noisy image “Woman” [1] by different methods. The images are better to be zoomed in on screen.

324



(a) Noisy [1]

(b) CBM3D [3, 4]

(c) WNNM [5]

(d) MLP [6]

325



(e) TNRD [7]

(f) NI [8]

(g) NC [1, 9]

(h) Ours

326

327

328

329

330

331

332

333

334

335

336

337

338

339

340

341

342

343

344

345

346

347

348

349

350

351

352

353

354

355

356

357

358

359

360

361

362

363

364

365

366

367

368

369

370

371

372

373

374

375

376

377

378

379

380

381

382

383

384

385

386

387

388

389

390

391

392

393

394

395

396

397

398

399

400

401

402

403

404

405

406

407

408

409

410

411

412

413

414

415

416

417

418

419

420

421

422

423

424

425

426

427

428

429

430

431

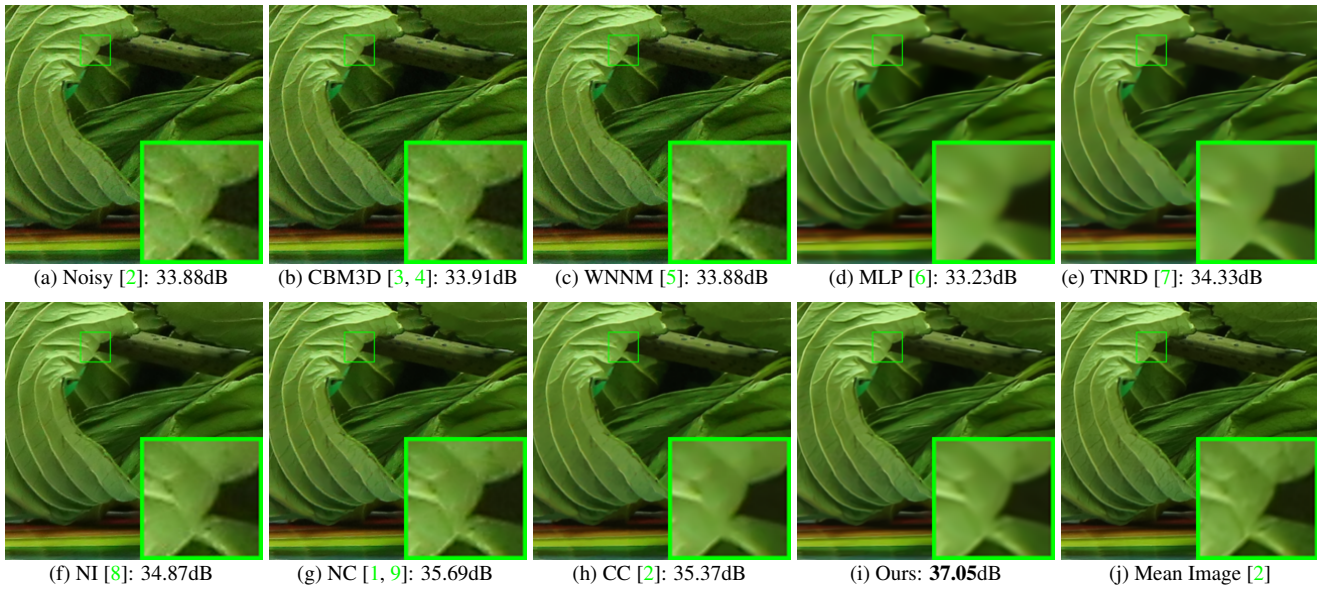


Figure 5. Denoised images of a region cropped from the real noisy image ‘Canon 5D Mark 3 ISO 3200 2’ [2] by different methods. The images are better to be zoomed in on screen.

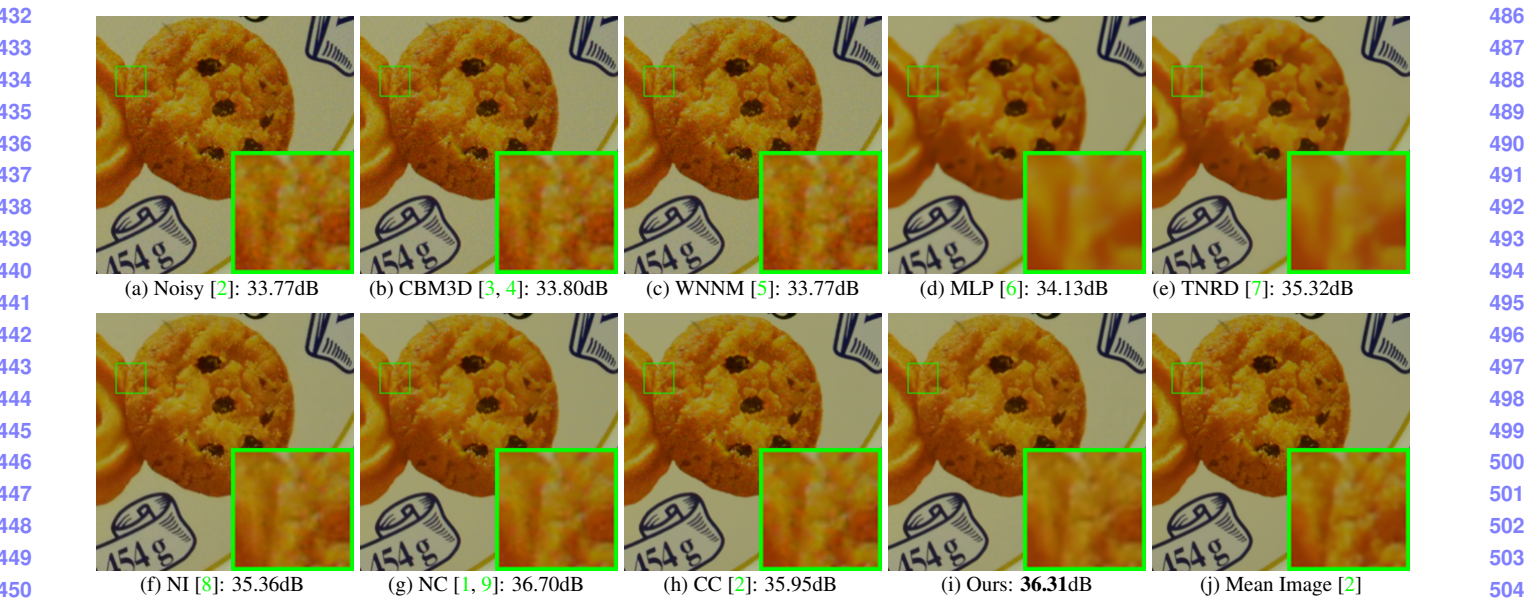


Figure 6. Denoised images of a region cropped from the real noisy image “Canon 5D Mark 3 ISO 3200 2” [2] by different methods. The images are better to be zoomed in on screen.

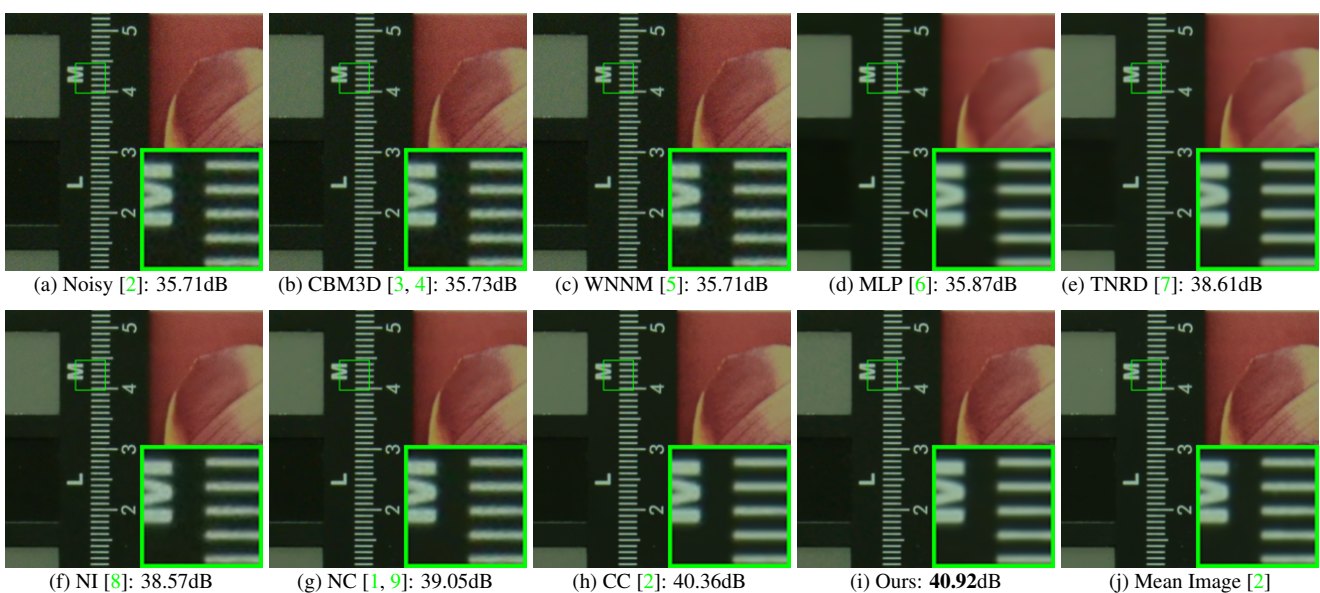


Figure 7. Denoised images of a region cropped from the real noisy image “Nikon D800 ISO 1600 2” [2] by different methods. The images are better to be zoomed in on screen.

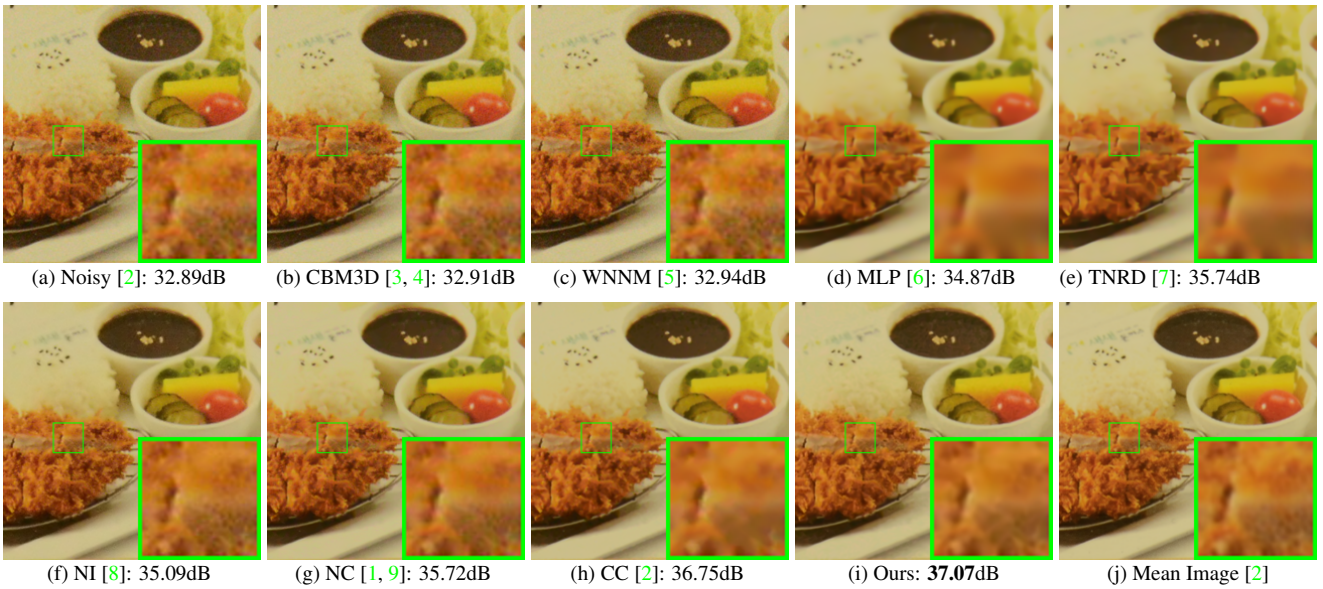


Figure 8. Denoised images of a region cropped from the real noisy image “Nikon D800 ISO 3200 2” [2] by different methods. The images are better to be zoomed in on screen.

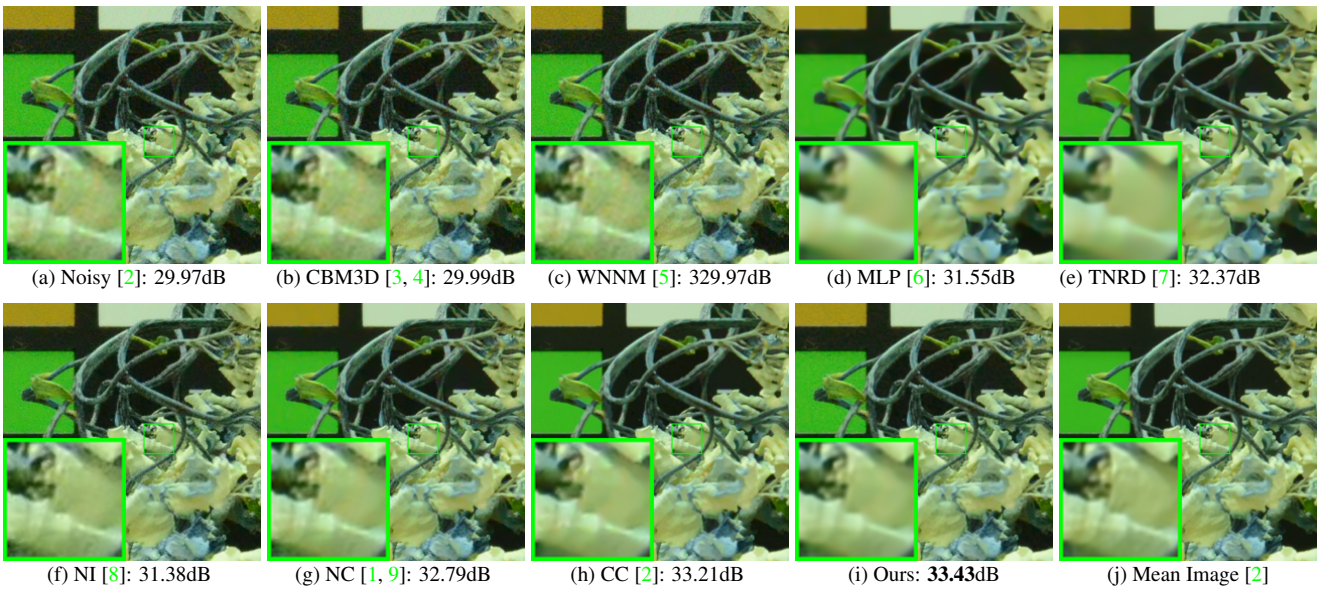
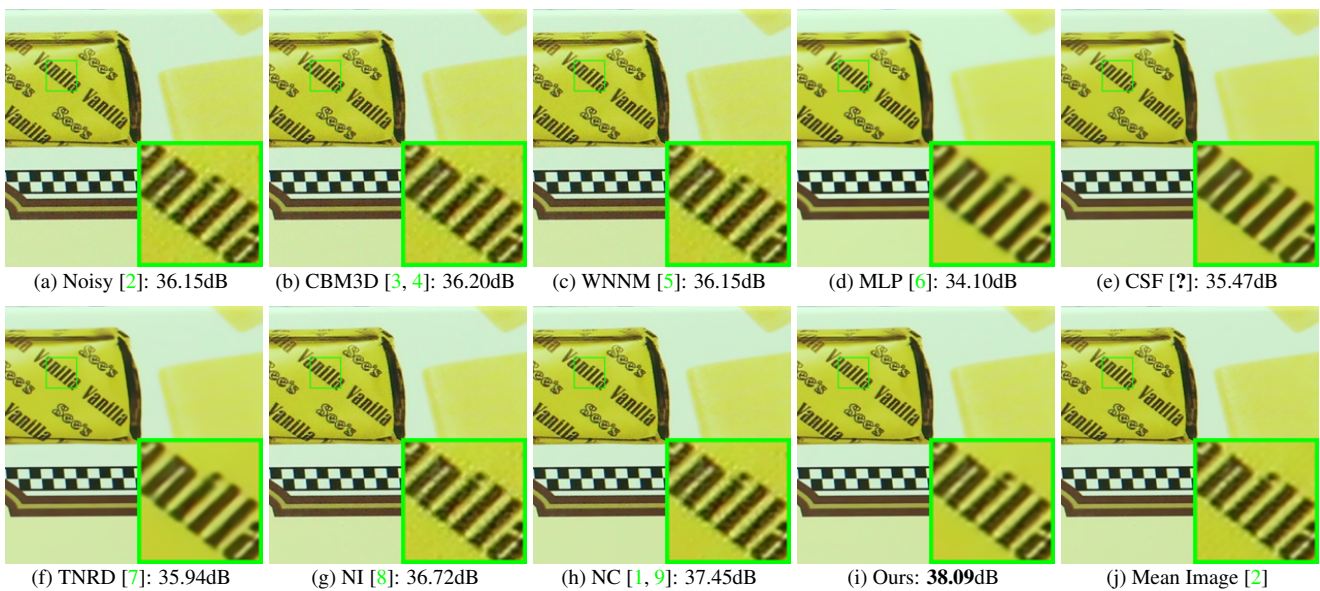


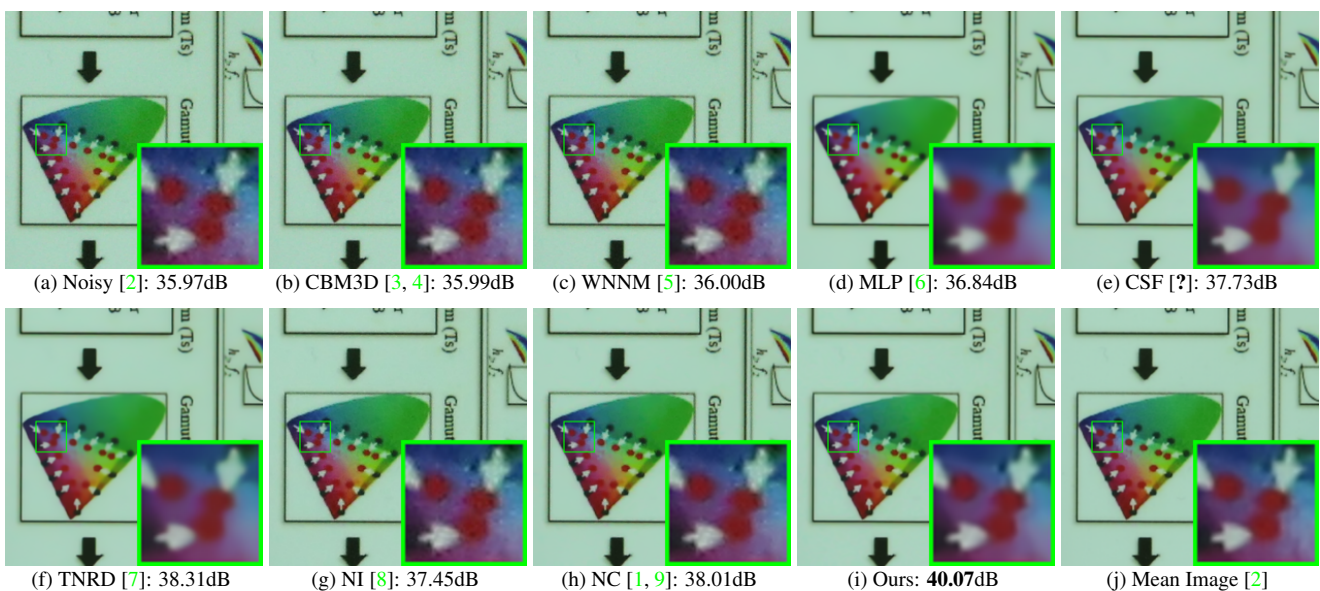
Figure 9. Denoised images of a region cropped from the real noisy image “Nikon D800 ISO 6400 2” [2] by different methods. The images are better to be zoomed in on screen.

#### 4. More Results on the 60 Cropped Images in [2]

In this section, we provide more visual comparisons of the proposed method with the state-of-the-art denoising methods on the 60 cropped real noisy images we cropped from [2]. As can be seen from Figures 10-15, on most cases, our proposed method achieves better performance than the competing methods. This validates the effectiveness of our proposed external prior guided internal prior learning framework for real noisy image denoising.



667  
668  
Figure 10. Denoised imagesupp of a region cropped from the real noisy image “Canon EOS 5D Mark3 ISO 3200 C1” [2] by different  
methods. The images are better viewed by zooming in on screen.



690  
691  
Figure 11. Denoised imagesupp of a region cropped from the real noisy image “Canon EOS 5D Mark3 ISO 3200 C2” [2] by different  
methods. The images are better viewed by zooming in on screen.

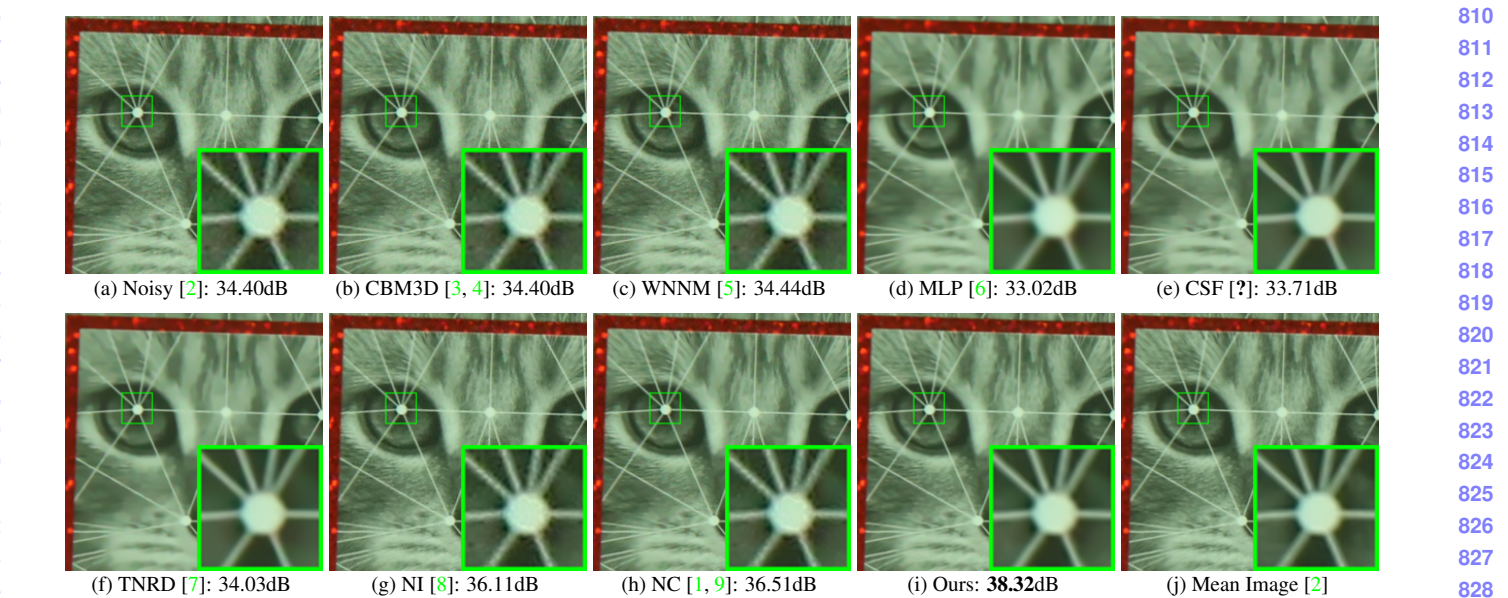


Figure 12. Denoised imagesupp of a region cropped from the real noisy image “Canon EOS 5D Mark3 ISO 3200 C3” [2] by different methods. The images are better viewed by zooming in on screen.

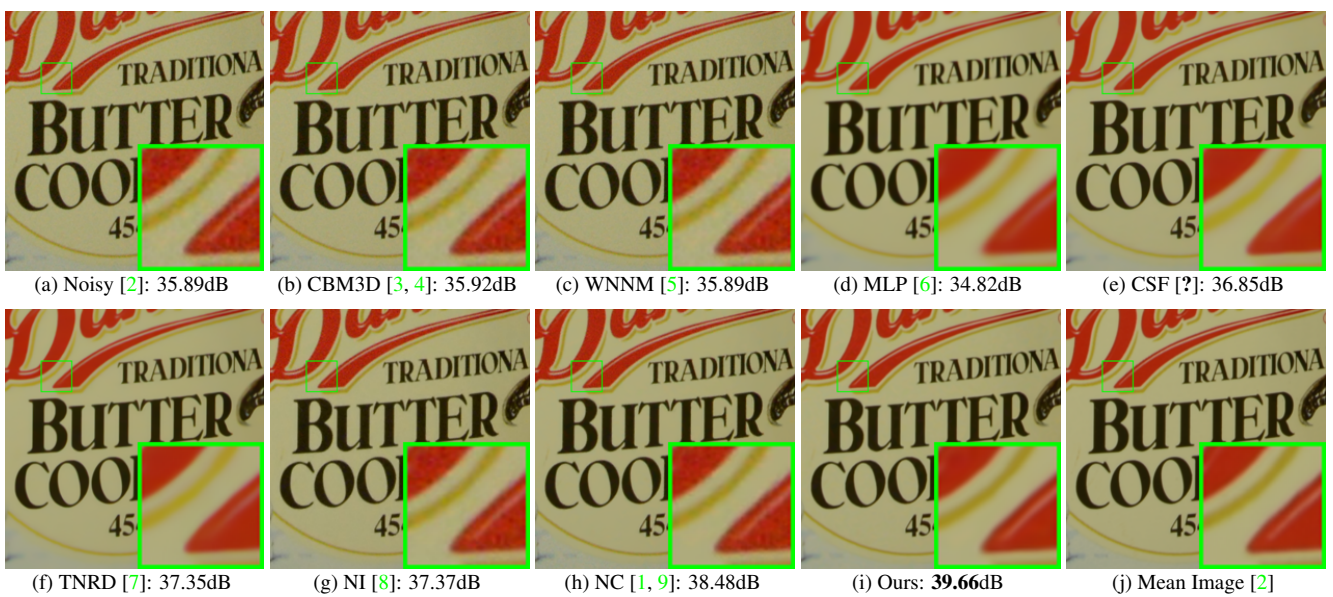


Figure 13. Denoised imagesupp of a region cropped from the real noisy image “Nikon D600 ISO 3200 C1” [2] by different methods. The images are better viewed by zooming in on screen.

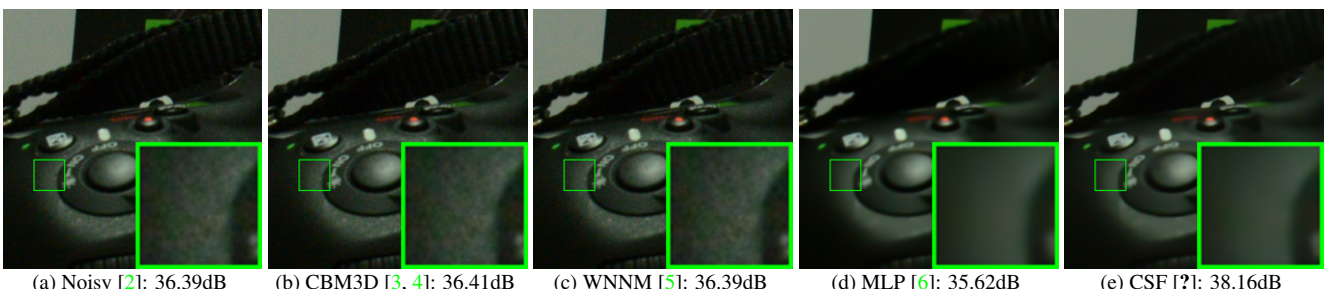


Figure 14. Denoised imagesupp of a region cropped from the real noisy image “Nikon D600 ISO 3200 C2” [2] by different methods. The images are better viewed by zooming in on screen.

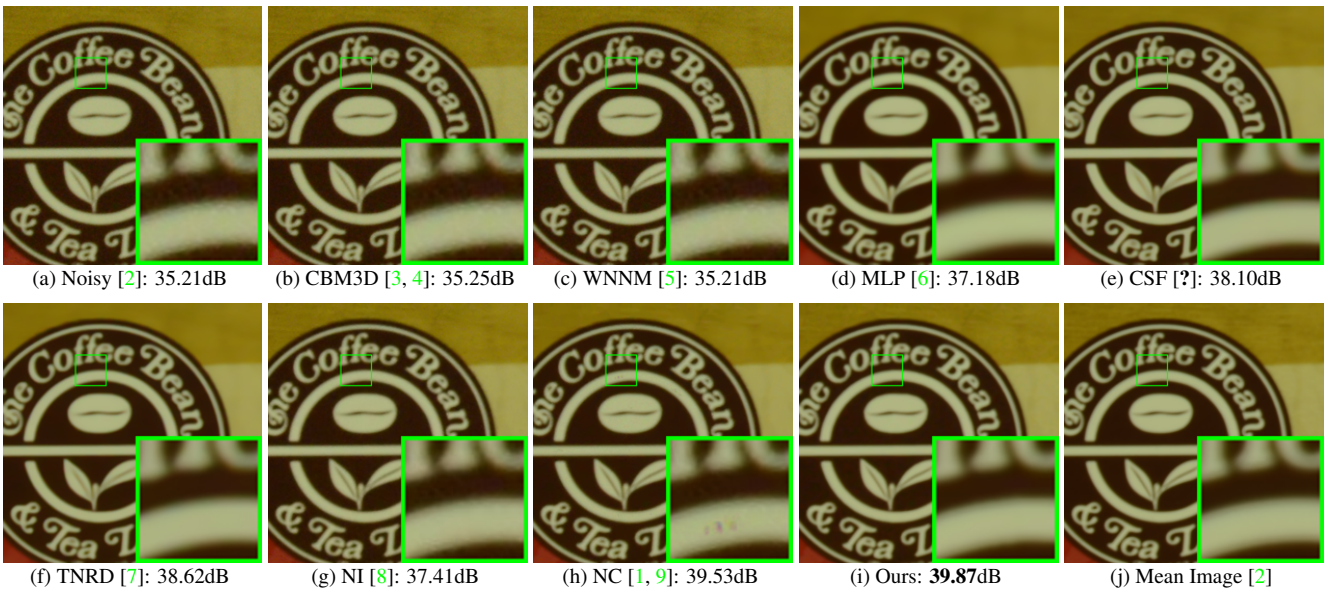


Figure 15. Denoised imagesupp of a region cropped from the real noisy image “Nikon D800 ISO 1600 B2” [2] by different methods. The images are better viewed by zooming in on screen.

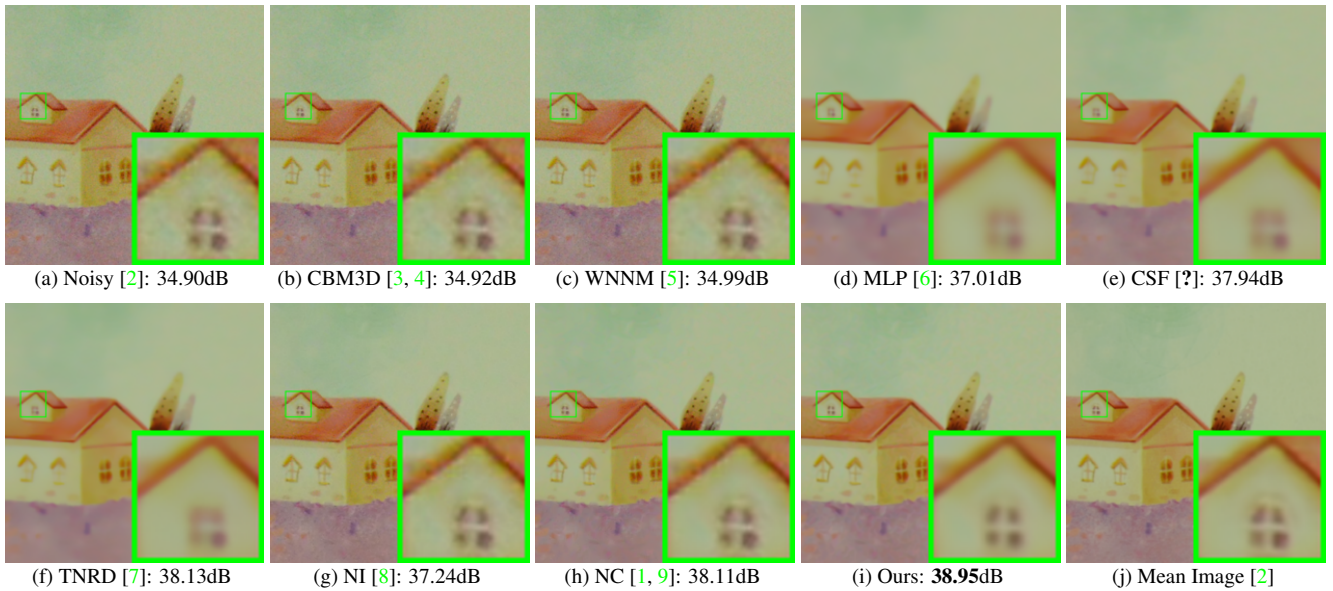


Figure 17. Denoised images of a region cropped from the real noisy image “Nikon D800 ISO 3200 A2” [2] by different methods. The images are better viewed by zooming in on screen.

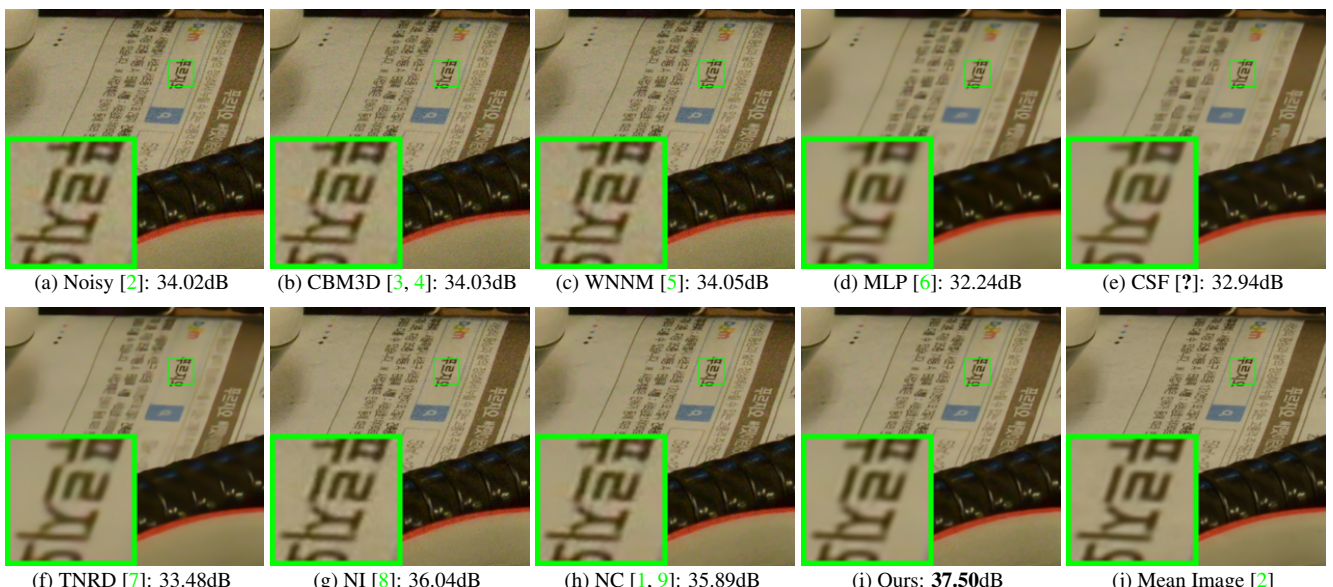


Figure 16. Denoised images of a region cropped from the real noisy image “Nikon D800 ISO 3200 A1” [2] by different methods. The images are better viewed by zooming in on screen.

## References

- [1] M. Lebrun, M. Colom, and J. M. Morel. The noise clinic: a blind image denoising algorithm. <http://www.ipol.im/pub/art/2015/125/>. Accessed 01 28, 2015. 1, 2, 3, 4, 5, 6, 7, 8, 9, 10, 11, 12
- [2] S. Nam, Y. Hwang, Y. Matsushita, and S. J. Kim. A holistic approach to cross-channel image noise modeling and its application to image denoising. *IEEE Conference on Computer Vision and Pattern Recognition (CVPR)*, pages 1683–1691, 2016. 1, 4, 5, 6, 7, 8, 9, 10, 11, 12
- [3] K. Dabov, A. Foi, V. Katkovnik, and K. Egiazarian. Image denoising by sparse 3-D transform-domain collaborative filtering. *IEEE Transactions on Image Processing*, 16(8):2080–2095, 2007. 2, 3, 4, 5, 6, 7, 8, 9, 10, 11, 12



Figure 18. Denoised imagesupp of a region cropped from the real noisy image “Nikon D800 ISO 3200 A3” [2] by different methods. The images are better viewed by zooming in on screen.

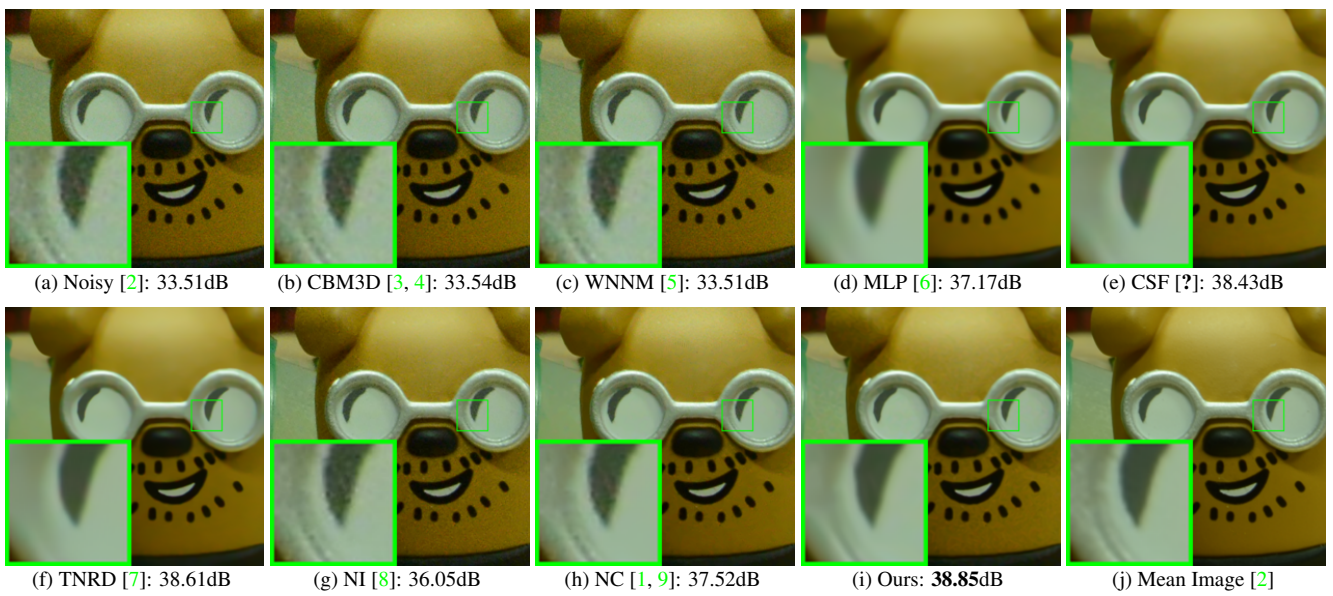


Figure 19. Denoised imagesupp of a region cropped from the real noisy image “Nikon D800 ISO 3200 A4” [2] by different methods. The images are better viewed by zooming in on screen.

- [4] K. Dabov, A. Foi, V. Katkovnik, and K. Egiazarian. Color image denoising via sparse 3D collaborative filtering with grouping constraint in luminance-chrominance space. *IEEE International Conference on Image Processing (ICIP)*, pages 313–316, 2007. 2, 3, 4, 5, 6, 7, 8, 9, 10, 11, 12
- [5] S. Gu, L. Zhang, W. Zuo, and X. Feng. Weighted nuclear norm minimization with application to image denoising. *IEEE Conference on Computer Vision and Pattern Recognition (CVPR)*, pages 2862–2869, 2014. 2, 3, 4, 5, 6, 7, 8, 9, 10, 11, 12
- [6] H. C. Burger, C. J. Schuler, and S. Harmeling. Image denoising: Can plain neural networks compete with BM3D? *IEEE Conference on Computer Vision and Pattern Recognition (CVPR)*, pages 2392–2399, 2012. 2, 3, 4, 5, 6, 7, 8, 9, 10, 11, 12
- [7] Y. Chen, W. Yu, and T. Pock. On learning optimized reaction diffusion processes for effective image restoration. *IEEE Conference on*

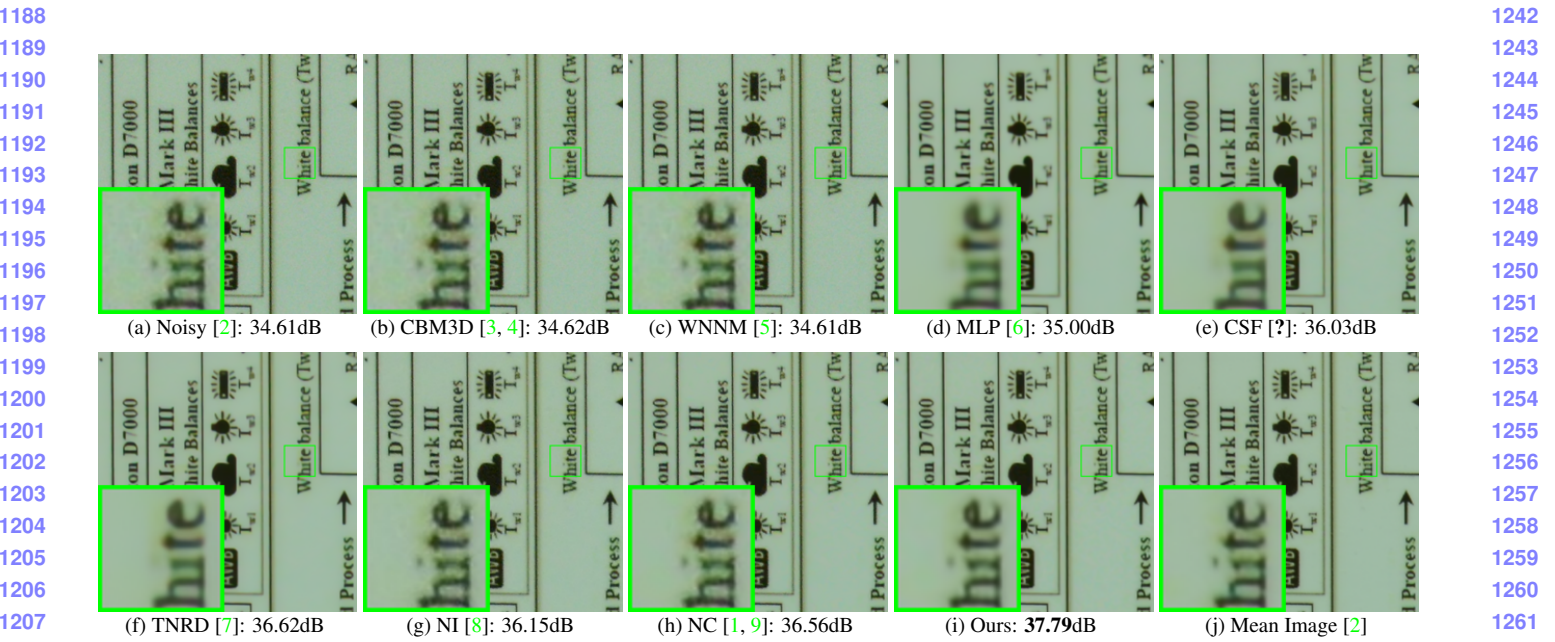


Figure 20. Denoised images supp of a region cropped from the real noisy image “Nikon D800 ISO 3200 A5” [2] by different methods. The images are better viewed by zooming in on screen.

*Computer Vision and Pattern Recognition (CVPR)*, pages 5261–5269, 2015. 2, 3, 4, 5, 6, 7, 8, 9, 10, 11, 12

[8] Neatlab ABSoft. Neat Image. <https://ni.neatvideo.com/home>. 2, 3, 4, 5, 6, 7, 8, 9, 10, 11, 12

[9] M. Lebrun, M. Colom, and J.-M. Morel. Multiscale image blind denoising. *IEEE Transactions on Image Processing*, 24(10):3149–3161, 2015. 2, 3, 4, 5, 6, 7, 8, 9, 10, 11, 12

1188  
1189  
1190  
1191  
1192  
1193  
1194  
1195  
1196  
1197  
1198  
1199  
1200  
1201  
1202  
1203  
1204  
1205  
1206  
1207  
1208  
1209  
1210  
1211  
1212  
1213  
1214  
1215  
1216  
1217  
1218  
1219  
1220  
1221  
1222  
1223  
1224  
1225  
1226  
1227  
1228  
1229  
1230  
1231  
1232  
1233  
1234  
1235  
1236  
1237  
1238  
1239  
1240  
1241

1242  
1243  
1244  
1245  
1246  
1247  
1248  
1249  
1250  
1251  
1252  
1253  
1254  
1255  
1256  
1257  
1258  
1259  
1260  
1261  
1262  
1263  
1264  
1265  
1266  
1267  
1268  
1269  
1270  
1271  
1272  
1273  
1274  
1275  
1276  
1277  
1278  
1279  
1280  
1281  
1282  
1283  
1284  
1285  
1286  
1287  
1288  
1289  
1290  
1291  
1292  
1293  
1294  
1295